AIAA JOURNAL
Vol. 41, No. 4, April 2003

Technical Notes

TECHNICAL NOTES are short manuscripts describing new developments or important results of a preliminary nature. These Notes cannot exceed six manuscript pages and three figures; a page of text may be substituted for a figure and vice versa. After informal review by the editors, they may be published within a few months of the date of receipt. Style requirements are the same as for regular contributions (see inside back cover).

Experimental Study of Corotating Wake-Vortex Merger at Reynolds Numbers of Order 10^5

R. L. Bristol,* J. M. Ortega,† and Ö. Savaş‡
University of California at Berkeley, Berkeley, California 94720-1740

Introduction

THE wake-vortex system trailing an aircraft is a major factor in airport operations, from both safety and capacity perspectives.[1,2] The wake of a conventional aircraft begins as a set of multiple vortices,[3] eventually merging to become a single pair of counter-rotating vortices. We model the near wake by two symmetric pairs of corotating vortices produced by a wing with a single, symmetric flap.[4,5] In addition to providing an example of the near-wake merger, this problem is important for efforts aimed at reducing the wake-vortex hazard during takeoffs and landings. For example, perturbations introduced at the wing to excite instabilities in the downstream single vortex pair must survive the multiple-vortex near wake.

Employing a linear stability analysis similar to that of Crow,[6] Jimenez[7] has found that a pair of equal-strength corotating vortices is stable to long-wavelength displacement perturbations. Klein et al.,[8] in an analysis that includes some nonlinear effects, did not find instabilities for a corotating pair. Crouch[9] presented an analysis of instabilities produced in a wake consisting of two pairs of corotating vortices, a configuration much like that of the present study. In addition to the Crow[6] instability, Crouch[9] found new instabilities with similar growth rates. However, these instabilities assumed a periodic, orbital background state, which makes it difficult to compare to the present case in which the vortices merge in about one orbit.

In the tow tank measurements of Refs. 4 and 5, nearly parallel corotating tip and flap vortices were observed to merge within one orbit, even for vortices beyond the critical two-dimensional merger separation distance. Evidence of vortex stretching was seen in the particle-induced velocimetry (PIV) data. These results suggested that three-dimensional effects were likely playing an important role in the flow, despite the lack of direct observations. The current study partially fills this gap with flow-visualization experiments and PIV measurements. In addition, the circulation-based Reynolds numbers Re_Γ for the present study have been increased by an order of magnitude.

Setup

The wake vortices were produced behind wings towed in a tank, which measures 70 m in length by 2.4 m in width by 1.5 m in water depth. Wings were formed by rolling sheet metal to a 17-cm-radius circular camber and tapering the leading and trailing edges. The wings' span is $b = 40$ cm, and the chord $c = 6.7$ cm. Four planforms were used, consisting of single, symmetric flaps of depth 2.2 cm and span widths 67, 50, 33, and 0% (unflapped). Two types of wings were used, differing in their respective thickness of 2.0 and 3.2 mm. The thicker wings had internal channels to allow for the injection of dye into the vortices. We refer to the two wing types as solid and channeled, respectively. The angle of attack of the wing, α, was set at either 3 or 4 deg. The towing speed U varied from 1 to 6 m/s.

The vortices were made visible by releasing fluorescent dye through small tubes at the tip and flap edges of the channeled wing. The low-pressure cores of the vortices were able to draw in a sufficient amount of dye. Blue light, covering the absorption peak of the dye, was used to illuminate the test section volume, covering a region of about $4 \times 2 \times 2.5$ m^3. Flow images were captured by five video cameras. In particular, orthogonal side and top views were taken to make wavelength measurements off the dye streaks. The dye remained concentrated along thin lines until just before merger, at which point it dispersed, leaving an ill-defined cloud. We use a right-handed coordinates system (x, y, z) attached to the wing: the x axis points into the wake, and the z axis is in the direction of the lift vector. Subscripts f and t refer to flap and tip vortices, respectively. Further details may be found in Refs. 10 and 11.

Results

As was done for similar wings in Refs. 4 and 5, we chose the Lamb–Oseen (Gaussian) vorticity distribution to model the subsequent vortices; $\omega_z(r) = (\Gamma_0/\pi\sigma^2)\exp(-r^2/\sigma^2)$, where Γ_0 is the circulation and r is the radial distance from the vorticity centroid $\boldsymbol{Y} = (Y, Z)$. Individually determined flap and tip vortex sizes, σ_f and σ_t, ranged between $0.047b$ and $0.052b$; hence, we take, for all flows, $\sigma = \sigma_f = \sigma_t \approx 0.05b = 2$ cm.

Figure 1 shows isovorticity surfaces for each of the four wing configurations, towed at $\alpha = 3$ deg and $U = 5$ m/s. The streamwise direction is in time converted, which may be converted to equivalent downstream distance as $x = Ut$. The physical aspect ratio of Fig. 1 is, thus, quite large; locally, the vortices are nearly parallel. The vorticity level is chosen to correspond to that found at a radius of 1.33σ of a Gaussian vorticity distribution fitted to the tip vortices. All vortex pairs complete approximately one orbit before they merge, as was seen in previous studies.[4,5] As was pointed out in Ref. 4, the orbital time and the characteristic time for the straining field both scale as d^2/Γ, where d is the separation between the two and Γ is the total vortex circulation for the pair. The rotation rate of pairs increases in time as they spiral inward, which is apparent as an increase in the helix pitch.

Figure 2 shows an example of the behavior of a vortex pair. As was observed by Chen et al.,[4] the centroid maintains a relatively straight vertical path (Fig. 2a) as the pair spiral around the common centroid, inward toward merger (Fig. 2b). The vector $\boldsymbol{R}(t) = [R(t), \theta(t)]$ connecting the centroids of the vortices (flap-to-tip) is shown in Fig. 2b and plotted in Fig. 2c. The angular velocity of the separation vector is nearly constant at 2.3 rad/s before the vortices merge. The separation of the two vortices $R(t)$ does not linearly decrease with

Received 6 December 2001; revision received 1 October 2002; accepted for publication 9 December 2002.

*Graduate Student, Department of Mechanical Engineering; currently Senior Engineer, Components Research, RA3-252, Intel Corp., 5200 Northeast Elam Young Parkway, Hillsboro, OR 97123. Member AIAA.

†Graduate Student, Department of Mechanical Engineering; currently Staff Scientist, New Technologies Engineering Division, Lawrence Livermore National Laboratory, P.O. Box 808 L-206, Livermore, CA 94551. Member AIAA.

‡Professor, Department of Mechanical Engineering; savas@me.berkeley.edu. Associate Fellow AIAA.

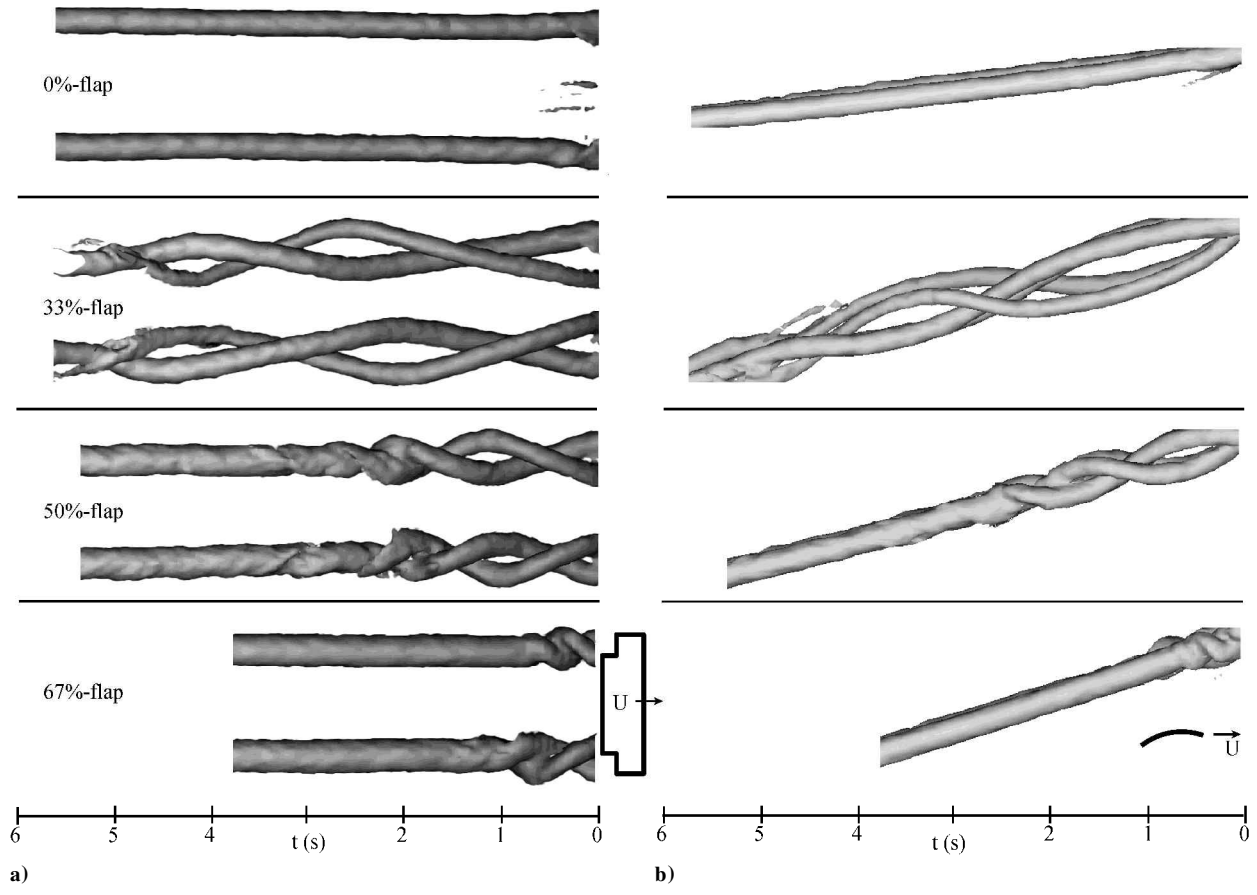

Fig. 1 Isovorticity surfaces for the wakes of four solid wings, $\alpha = 3$ deg and $U = 5$ m/s: a) from below with the wing flying overhead and b) side view.

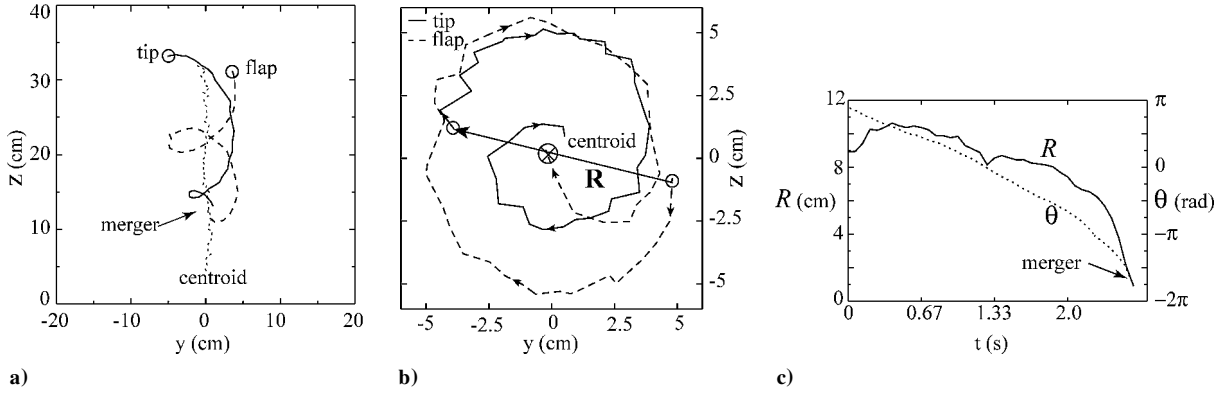

Fig. 2 Vortex trajectories, $\Gamma_f + \Gamma_t = 1390$ cm^2/s, $\Gamma_t/\Gamma_f = 0.84$, $d = 10$ cm, and merger at 2.6 s, or at 0.9τ: a) laboratory reference frame, b) with respect to centroid of the pair, and c) separation vector $R = (R, \theta)$.

time, but wavers before they merge. The initial increase is due to the rollup of the vortices, whereas the first "hump" (from $t = 0$ to 1.3 s) is consistent with the ideal behavior of a four-vortex system, in which the flap vortices initially descend rapidly due to the influence of the opposite pair. Because of these fluctuations, the geometric separation between the tip and flap edges of the wing is used as a representative tip–flap distance d. For the 33, 50, and 67% flap wings, d is, thus, 13.3, 10.0, and 6.7 cm, respectively.

Merger was defined to occur once the vortex centroids came within 1σ. As was done by Chen et al.,[4] the merger times are measured in terms of the orbital period $\tau = 4\pi^2 d^2/(\Gamma_f + \Gamma_t)$. For example, for the 50% flap vortex pair of Fig. 2, $\tau = 2.84$ s, giving an orbital angular velocity of $2\pi/\tau = 2.21$ rad/s, which is in good agreement with the slope of Fig. 2c. The merger time for this pair is 0.9τ. Merger consistently occurs in about one orbit period for all of the speeds and angles of attack studied here. Although the merger times for the 67% wings were somewhat less than one orbit, this case was somewhat exceptional because the vortices began merging nearly from the moment they were formed.

The merger behavior cannot be explained from a two-dimensional perspective. The separation of the vortices in terms of the core sizes for the 33 and 50% cases are larger than those that would allow for merger in one orbit in a two-dimensional dimensional case,[12] even accounting for the particular vortex size, distribution, and Reynolds numbers studied here.[10] This alone would lead us to suspect that the merger was a three-dimensional process, but in fact direct signatures of three-dimensional behavior has been seen in the PIV data.[4] The evidence of this was in strong fluctuations in the moments of vorticity, which should have been conserved if the flow were truly two-dimensional. However, the PIV data are unable to show

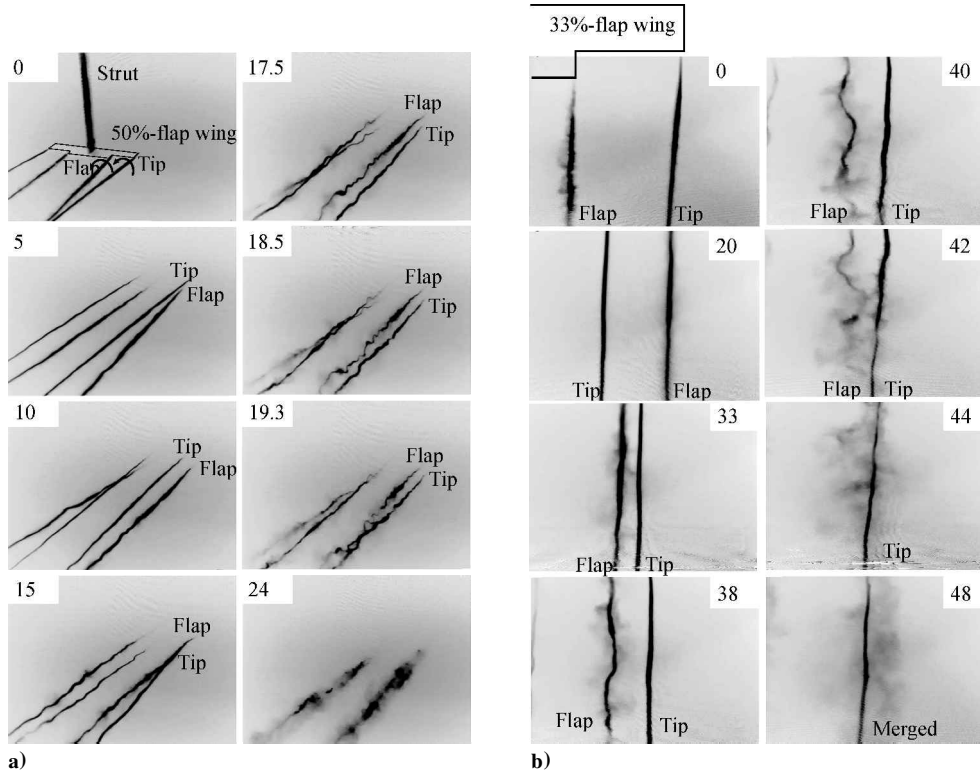

Fig. 3 Flow visualization: a) oblique view of wake of 50% flap wing, 0−24 *Ut/b* and b) overhead view of one-half of wake of 33% flap wing, 0−48 *Ut/b*.

explicitly the precise three-dimensional form of these interactions. These became evident with the volumetric flow visualizations.

Figure 3 shows two sample flow visualization sequences for the 50 and 33% flap wings. Figure 3a shows several pictures from a submerged camera looking down the length of the tank and offset to one side. As the vortices complete one orbit, a sinuous disturbance appears on the flap vortex and to a lesser extent on the tip vortex. The dye then disperses as the vortices merge. In Fig. 3b, a disturbance again appears on the flap vortex and to a minor extent on the tip vortex. The disturbance first appears near the three-quarter orbit point and grows until the two merge.

The wavelength λ, amplitude, and orientation of the disturbances were estimated using the orthogonal video images. Wavelengths were found from the average distance between the peaks of the disturbances. The component of the amplitudes in each of the two projections was found from the mean displacement of the peaks and troughs. The disturbance was found to lie roughly in a plane, as verified in the nonorthogonal views. The angle of the plane of the disturbance was determined by taking the arctangent of the ratio of the vertical projection of the amplitude with the horizontal one. These measurements were made manually using digitized versions of the images, thus, requiring some judgment as to the positions of the peaks and troughs. In many images, such as those in Fig. 3b, the peaks and troughs of the disturbance were clearly identifiable. They were not so clear in other cases, such as when one vortex occluded another or when the amplitude of the disturbance was small. The measured dimensionless wave numbers, $k\sigma = 2\pi\sigma/\lambda$, of the disturbance for the 33 and 50% flap wing configurations are 1.0 and 1.3, respectively. Data are not accessible for the 67% flap wing, although this case also displayed a sinuous disturbance. However, because the vortices were in the process of merging nearly from the moment they first appeared, the dye did not entrain sharply, resulting in a somewhat clouded picture.

The three-dimensional appearance of the disturbances occurred in every run just before merger. These disturbances provide a means for vortices to merge despite their relatively large separation. As the disturbance grows in magnitude, the vortices are periodically brought together in close proximity, initiating regions of strong interactions between the two. At a large enough amplitude, these regions may come within the critical separation for two-dimensional merger, providing a strong means for the two vortices to link. However, this simple view misses other possible effects, in particular the mechanisms by which the two vortices begin to link before merger. Such interactions are difficult to discern from the action of a passive dye.

The disturbances grow at an angle of roughly 45 deg with respect to the tip vortex. This is consistent with growth driven by the strain field from the tip vortex. As illustrated by Widnall et al.[13] for the case of an equal-strength, oppositely rotating pair, such a velocity field produces a straining field with an extensional axis at 45 deg with respect to the line joining the two vortices. Planar perturbations can then grow in this straining field. However, such perturbations will also tend to self-induce and rotate about the vortex. Instability occurs if the self-induced rotation of the perturbation is weaker than the peak azimuthal component of the straining field. For a Rankine vortex, Widnall et al. show how this can occur not only for a simple perturbation in vortex position, but also for one with a radial node, in which the interior and exterior of the vortex move in opposite directions. This is analogous to the "elliptic instability" of solid-body rotation in a straining field. The self-rotation of such a mode vanishes at a wave number of approximately 2.5 vortex radii, which allows for maximum growth of the perturbation along the extensional axis of the straining field. This wave number corresponds to a wavelength of 2.5 vortex radii, earning the name short-wave instability because it is much shorter than that of the classic Crow[6] instability arising from displacement perturbations. For Gaussian vortices, Eloy and Le Dizes[14] have demonstrated the elliptic mode in a straining field to be most unstable at a wavelength of 2.26σ.

For the corotating vortices studied here, the situation is somewhat different because the unperturbed state of such a pair is not to descend downward, but to rotate about a common centroid. The implications of this are investigated in Ref 10. The general result is that a corotating pair is stable to displacement perturbations, which is consistent with the results of Jimenez[7] and Klein et al.[8] However, such a pair can still be destabilized by an elliptic perturbation, although at somewhat longer wavelengths than for the nonrotating case of Eloy and Le Dizes.[14] For the 33 and 50% cases studied in the flow visualization here, the wave numbers of maximum linear instability are found in Ref. 10 to occur at 1.9σ and 1.7σ, respectively.

These numbers are within a factor of two of those observed here. Given the experimental uncertainties of the parameters used in the calculations, and the simplicity of the model used (a single pair of parallel, Gaussian vortices), this approximate agreement is encouraging. Higher resolution PIV data could directly confirm or deny the presence of the elliptic mode in these vortices, by showing if the core and the periphery were displaced relative to each other. An elliptic instability was in fact demonstrated this way by Leweke and Williamson[15] for an equal-strength counter-rotating pair at $Re_\Gamma \approx 3 \times 10^3$.

Conclusions

Corotating tip–flap vortex pairs are studied at Re_Γ of order 10^5. The evolution of the velocity field at a fixed cross section is recorded, yielding measures of the circulation ratio, separation, and vortex size. The pair is observed to merge within about one orbital period. Flow visualization clearly shows the three-dimensional nature of this process, with the appearance of strong sinuous disturbances on the weaker flap vortex, and to a lesser extent on the tip vortex. The wave number of this disturbance and its alignment with the extensional axis of the straining field from the partner vortex suggest it to be an example of an elliptical instability. For such an instability driven by the straining field of the partner vortex, the growth rate scales as the inverse of the square of the vortex separation, $1/d^2$. This growth rate matches the scaling of the orbit period, thus, yielding finite amplitudes within one orbit. This provides an explanation for the observed merger in about one orbit, even for vortices spaced too far apart to merge in two dimensions.

Acknowledgments

R. L. Bristol and J. M. Ortega acknowledge the support of the National Science Foundation Graduate Fellowship program during the course of this research.

References

[1]Donaldson, C., and Bilanin, A., "Vortex Wakes of Conventional Aircraft," AGARDograph 204, edited by R. H. Korkegi, May 1975.

[2]Rossow, V. J., "Lift-Generated Vortex Wakes of Subsonic Transport Aircraft," *Progress in Aerospace Sciences*, Vol. 35, No. 6, 1999, pp. 507–660.

[3]Ciffone, D., and Lonzo, C., "Flow Visualization of Vortex Interactions in Multiple Vortex Wakes Behind Aircraft," NASA TM X-62, 459, June 1975.

[4]Chen, A. L., Jacob, J. D., and Savaş, Ö., "Dynamics of Corotating Vortex Pairs in the Wakes of Flapped Airfoils," *Journal of Fluid Mechanics*, Vol. 382, 1999, pp. 155–193.

[5]Bristol, R. L., Ortega, J. M., and Savaş, Ö., "A Towing Tank Study of Airfoil Wake Vortices at Re_Γ of Order 10^5," AIAA Paper 99-3419, June 1999.

[6]Crow, S. J., "Stability Theory for a Pair of Trailing Vortices," *AIAA Journal*, Vol. 8, No. 12, 1970, pp. 2172–2179.

[7]Jimenez, J., "Stability of a Pair of Co-Rotating Vortices," *Physics of Fluids*, Vol. 18, No. 11, 1975, pp. 1580–1581.

[8]Klein, R., Majda, A. J., and Damodaran, K., "Simplified Equations for the Interaction of Nearly Parallel Vortex Filaments," *Journal of Fluid Mechanics*, Vol. 288, 1995, pp. 201–248.

[9]Crouch, J. D., "Instability and Transient Growth for Two Trailing-Vortex Pairs," *Journal of Fluid Mechanics*, Vol. 350, 1997, pp. 311–330.

[10]Bristol, R. L. "Co-operative Wake Vortex Instabilities," Ph.D. Dissertation, Dept. of Physics, Univ. of California, Berkeley, CA, Dec. 2000.

[11]Ortega, J. M., Bristol, R. L., and Savaş, Ö., " Experimental Study of the Instability of Unequal-Strength Counter-Rotating Vortex Pairs," *Journal of Fluid Mechanics*, Vol. 474, 2003, pp. 35–84.

[12]Rossow, V. J., "Convective Merging of Vortex Cores in Lift-Generated Wakes," *Journal of Aircraft*, Vol. 14, No. 3, 1977, pp. 283–290.

[13]Widnall, S. E., Bliss, D., and Tsai, C., "The Stability of Short Waves on a Vortex Ring," *Journal of Fluid Mechanics*, Vol. 66, No. 1, 1974, pp. 35–47.

[14]Eloy, C., and Le Dizes, S., "Three-Dimensional Instability of Burgers and Lamb–Oseen Vortices in a Strain Field," *Journal of Fluid Mechanics*, Vol. 378, 1999, pp. 145–166.

[15]Leweke, T., and Williamson, C. H. K., "Cooperative Elliptic Instability of a Vortex Pair," *Journal of Fluid Mechanics*, Vol. 360, 1998, pp. 85–119.

A. Plotkin
Associate Editor

Reynolds-Number Correlations for Separation of Turbulent Boundary Layers

V. A. Sandborn*
Colorado State University, Fort Collins, Colorado 80521

Introduction

A PHYSICAL model for turbulent boundary-layer separation was proposed by Sandborn and Kline,[1] as a transition region from unseparated to separated flow. Correlations were developed to indicate the onset of intermittent and zero-mean surface shear stress, $\bar{\tau}_w = 0$ separations, in terms of the velocity profile shape factor H and the ratio of displacement to boundary-layer thickness δ^*/δ. The intermittent separation location was taken as the point where the adverse effects associated with flow separation are present and viscous constraints are no longer important. It is the location most researchers identify by flow visualization as turbulent separation, and the point most often predicted by analytical studies. Sandborn and Liu[2] demonstrated that the $\bar{\tau}_w = 0$ separation was equivalent to laminar boundary-layer separations.

The present Note demonstrates that the separation correlations of Sandborn and Kline can be recast in terms of the Reynolds number instead of the less well-defined boundary-layer thickness.

Separation Correlations

Figure 1 shows the curves obtained when the Sandborn–Kline correlations are recast in terms of R_θ. Extrapolated values of form factor and Reynolds number were determined for each set of data points where they crossed the original Sandborn–Kline correlation curves. (See Sandborn and Kline[1] for references to the experimental data.) Most of the variation of H with R_θ occurs for values of R_θ less than 2×10^4. For values of R_θ greater than 2×10^4, the variation of H is quite small ($H \approx 2.5 + 0.2$ for intermittent separation and $H \approx 3.8 + 0.1$ for $\bar{\tau}_w = 0$). The $\bar{\tau}_w = 0$ curve was reported previously.[3]

The compressible flow values (local Mach number ~0.33 and 0.59) of H and R_θ shown on Fig. 1 are the incompressible transformed values (untailed) and the direct, mass flow values (tailed). The compressible measurements were made in a 10×15 cm, cross-section facility at the NASA Ames Research Center (see Sandborn and Seegmiller[4] for details of the basic facility). Details of the tunnel setup for the measurements in the 61×61 cm tunnel were given by Sandborn.[5]

Whereas the separation transition process begins with the first appearance of backflow, the cross-hatched region on Fig. 1 indicates the area where the major adverse problems associated with separation are present. The cross-hatched region corresponds to that part of the flow where the mean flow quantities overshadow the Reynolds turbulent terms.[2]

The fourth-power polynomial (computer fitting), shown in Fig. 1, was employed to estimate the value of the skin-friction coefficient for intermittent separation. Computed values of c_f at the location of intermittent separation are shown on Fig. 2.

To demonstrate the affect of Reynolds number on separation, a set of measurements were made in a small 8.9×16.5 cm inlet duct. The duct was expanded to 25.4 cm ($\delta/R \approx 0.02$) to produce

Received 7 July 2002; revision received 20 November 2002; accepted for publication 30 November 2002.

*Emeritus Professor, Department of Civil Engineering, Engineering Research Center; v.sandborn@attbi.com. Senior Member AIAA.